European Journal of Radiology 85 (2016) 1092–1098

Contents lists available at ScienceDirect

European Journal of Radiology

journal homepage: www.elsevier.com/locate/ejrad

Use of BI-RADS-MRI descriptors for differentiation between mucinous carcinoma and fibroadenoma

Takao Igarashi*, Hirokazu Ashida, Kazuhiko Morikawa, Kenji Motohashi, Kunihiko Fukuda

Department of Radiology, The Jikei University School of Medicine 3-25-8, Nishi-Shimbashi, Minato-ku, Tokyo 105-8461 Japan

ARTICLE INFO

Article history:
Received 3 January 2016
Received in revised form 11 March 2016
Accepted 16 March 2016

Keywords:
Breast
Mri
Mucinous carcinoma
Fibroadenoma

ABSTRACT

Objective: We evaluated the latest breast imaging reporting and data system (BI-RADS) magnetic resonance imaging (MRI) (5th edition) descriptors and non BI-RADS MRI factors that contribute to differentiation between mucinous carcinomas (MCs) and fibroadenomas (FAs).

Materials and methods: This retrospective study included 27 patients with P-MCs or M-MCs similar to P-MCs and 22 patients with FAs who underwent breast MRI between October 2008 and July 2014 at our institution. Definitive histopathological diagnoses were made for all of the MCs and FAs. The latest BI-RADS MRI descriptors for abnormal enhancement, including maximum diameter, shape (irregular or round/oval), margin (irregular or circumscribed), rim enhancement (present or absent), dark internal septation (absent or present), delayed internal enhancement (heterogeneous or homogeneous), and the time–intensity curve pattern (not persistent or persistent) were evaluated. As additional non BI-RADS MRI factors related to differentiation between MC and FA, age, signal intensity in the T2-weighted image (high or not high), extent of lobulation (strong or weak), enhancing internal septation (present or absent), and the apparent diffusion coefficient value were also evaluated. One radiologist retrospectively evaluated interpreted MR findings and analyzed the findings. Statistically significant findings were identified through univariate and multivariate analyses. Then, three blinded radiologists reviewed the MR images where MR findings had shown a significant association with outcomes during univariate analyses. Independently, the three blinded readers reviewed the MR images for the evaluation of inter-observer variability, and then arrived at a consensus for the evaluation of observer performance. Observer performance and inter-observer variability were determined via a receiver-operating-characteristic curve analysis and weighted k statistics. The sensitivity, specificity, and accuracy of each of the MR findings were calculated.

Results: Univariate analyses showed that irregular margins were observed more frequently in MCs than in FAs (11/27, 41% vs. 1/22, 0.5%, $p < 0.05$). MCs also showed rim enhancement, delayed heterogeneous enhancement, and enhancing internal septation more frequently than FAs ($p < 0.05$). FAs showed circumscribed margins more frequently than MCs (21/22, 95% vs. 16/27, 59%, $p < 0.05$). FAs also showed dark internal septation more frequently than MCs (18/22, 82% vs. 3/27, 11%, $p < 0.05$). In multivariate analyses, the most significant feature in lesion characterization was delayed heterogeneous enhancement. In the blinded reading, a combination of irregular margin and delayed heterogeneous enhancement showed the highest sensitivity (96.3%) and accuracy (87.8%). Enhancing internal septation showed the highest specificity (90.9%). The κ values with confidence ratings for differentiation between MCs and FAs were 0.63–0.67, which showed substantial agreement among the three radiologists.

Conclusions: The combination of irregular margin and delayed heterogeneous enhancement and enhancing internal septation were significant findings for differentiation between P-MC or M-MC similar to P-MC and FA.

Abbreviations: BI-RADS, breast imaging reporting and data system; MRI, magnetic resonance imaging; MC, mucinous carcinoma; FA, fibroadenoma; ADC, apparent diffusion coefficient; MMG, mammography; US, ultrasonography; AUC, area under the curve.

* Corresponding author.
E-mail address: igarashi-t@jikei.ac.jp (T. Igarashi).

http://dx.doi.org/10.1016/j.ejrad.2016.03.012
0720-048X/

1. Introduction

Mucinous carcinoma (MC) is a rare histological type of mammary neoplasm that is characterized by a large amount of mucin production [1–3]. The incidence of MC has been reported to be 1–6% for all primary breast cancers [1–3]. MC usually occurs in the elderly, and the median age at diagnosis is >55–60 years [1–3]. MCs are classified as pure MCs (P-MCs) and mixed MCs (M-MCs). P-MCs consist exclusively of tumor tissue with extracellular mucin production, and M-MCs are defined by the World Health Organization as tumors in which 50–90% of the area is mucinous and is admixing with infiltrating ductal epithelial components [1].

P-MCs show less aggressive behavior than do other invasive ductal carcinomas, metastasize to axillary lymph nodes less frequently than do M-MCs, and can be managed with less invasive surgery than can M-MCs [4]. Positive nodal status appears to be the most significant predictor of worse prognosis [1–3]. M-MCs with prominent invasive components are obviously different from FAs and easy to diagnose as malignancies. On the other hand, P-MCs and M-MCs similar to P-MCs show findings similar to those of FAs, with myxomatous or edematous changes on both mammography (MMG) and ultrasonography (US). The MMG and US findings reported for P-MCs tend to have benign characteristics [5]. One type of benign tumor confused with P-MCs is myxomatous fibroadenomas (FAs) [6]. Myxoid or edematous FAs and MCs visualized by magnetic resonance imaging (MRI) display high signal intensity (SI) on T2-weighted images within the lesion [7,8]. The high water content of the myxoid matrix may explain the lesions' increased SI on T2-weighted turbo spin-echo images [9]. T2-weighted SI is not a reliable factor in differentiation between MC and FA [9,10]. Among breast carcinomas that have long T2 relaxation times, MCs are common and occasionally difficult to distinguish from FAs on T2-weighted images alone [10]. Therefore, it is essential to confirm a diagnosis established on the basis of morphological and kinetic features on dynamic contrast-enhanced MRI (CEM) in addition to T2-weighted images. Reliable descriptors for differentiation of P-MCs or M-MCs similar to P-MCs and FAs can be used to reduce the number of unnecessary needle biopsies or partial resections and enable early detection of MCs without metastasis. There are only a few reports on differentiation between P-MCs or M-MCs similar to P-MCs and FAs by MRI, and to our knowledge, no studies have used the latest breast imaging reporting and data system (BI-RADS) MRI (5th edition) descriptors for differentiation [11].

The purpose of the present study was to determine reliable BI-RADS MRI descriptors and non BI-RADS MRI factors that contribute to differentiation between P-MCs or M-MCs similar to P-MCs and FAs.

2. Materials and methods

2.1. Patients

This retrospective study was approved by the Committee on Clinical Studies at our institution (the approval number, 27-044). The requirement of informed consent was waived. Among 2500 patients who underwent breast CEM imaging between October 2008 and July 2014 at our institution, 27 patients with P-MCs or M-MCs similar to P-MCs and 22 patients with FAs who were histopathologically diagnosed were enrolled. Most of the patients were examined for the purpose of qualitative diagnosis. We excluded patients who did not undergo surgery or core needle biopsy at our institution, received neoadjuvant chemotherapy, had poor MR image quality, or had M-MCs that had obvious invasive components on MR images. All of the patients with MCs (24 pure type, three mixed type) underwent surgical resection. All of the patients with FAs underwent core needle biopsy or surgical resection. All of the patients were female; their ages ranged from 23 to 78 years (mean, 53 years) in the patients with MCs and from 11 to 53 years (mean, 38 years) in the patients with FAs. The maximum diameters of the MCs ranged from 0.8 to 3.6 cm (mean, 2 cm) and those of the FAs ranged from 0.9 to 11 cm (mean, 3 cm).

2.2. MRI

MRI was performed on a 1.5-T system (Symphony®, Siemens Medical Solutions, Erlangen, Germany) using a maximum gradient field strength of 30 mT/m and a 4-ch CP breast array coil. All patients were examined in the prone position. First, coronal T2-weighted spectral attenuated inversion recovery images of both breasts were obtained by using the following parameters: repetition time (TR)/echo time (TE), 4000 ms/73 ms; flip angle,150°; field of view, 35 × 35 cm; matrix size, 806 × 896; slice thickness, 4 mm; gap, 0; number of excitations (NEX), 1. Subsequently, coronal DWIs of both breasts were obtained at b values of 0,1000, and 1500 s/mm^2 by using the following parameters: TR/TE, 5600 ms/87 ms; field of view, 35 × 35 cm; matrix size, 234 × 320; slice thickness, 3.5 mm; slice gap, 0; NEX, 5. Apparent diffusion coefficient (ADC) maps were automatically generated on the operating console by using the least squares method with all three images and b values of 0,1000 and1500 s/mm^2.Dynamic CEMs were acquired by using a three-dimensional fat-suppressed volumetric interpolated breath-hold examination sequence by using the following parameters: TR/TE, 5 ms/2.41 ms; flip angle, 15°; field of view, 340 mm; matrix, 768 × 768; receiver bandwidth, 340 kHz/pixel; mean partition thickness, 0.9 mm; time of acquisition, 85 s; NEX, 1. The section thickness varied depending on the size of the breast. Sections were acquired without a gap. Both breasts were included in the images. Three contrast-enhanced acquisitions centered at 60 s, 120 s, and 240 s after the start of the IV administration of 0.1 mmol/kg gadopentetate dimeglumine (Magnevist; Bayer Health Care) at a rate of 1 mL/s, followed by a 15 mL saline flush performed by using an automatic injector.

2.2.1. Interpretation of MR findings

All breast MR images had been initially interpreted at the time of clinical practice by one radiologist (T.I). In this study, the same radiologist with 14 years' experience in breast MR imaging retrospectively evaluated and interpreted the MR findings of the 49 histopathologically diagnosed lesions on a picture archiving and communication systems monitor and analyzed the findings. The BI-RADS MRI descriptors, including maximum diameter, shape (irregular or round/oval), margin (irregular or circumscribed), rim enhancement (present or absent), dark internal septation (absent or present), delayed internal enhancement (heterogeneous or homogeneous), the time–intensity curve pattern (not persistent or persistent) were evaluated and analyzed by the univariate analyses. In addition to the BI-RADS MRI descriptors, non BI-RADS MRI factors related to differentiation between MCs and FAs, including age, signal intensity in the T2-weighted image (high or not high), extent of lobulation (strong or weak), enhancing internal septation (present or absent), and ADC value, were also evaluated and analyzed by the univariate analyses. The extent of lobulation was classified into strong (acute angle) or weak (obtuse angle). The internal enhancement on delayed phase was classified as heterogeneous or homogeneous. The ADC measurements were performed on ADC maps. The region of interest was placed manually within the solid component of the lesion. At least three measurements were made for each lesion, and the lowest one was accepted as the ADC value. Then, three radiologists (H.A., K.M., and K.M. with 14, 9, and 7 years of experience, respectively, in interpreting body MR imaging, including breast MR) blinded to clinical and histopathological infor-

mation retrospectively reviewed the MR images that had shown a significant association with outcomes during the univariate analyses. Independently, the three blinded readers reviewed the MR images for the evaluation of inter-observer variability, and then arrived at a consensus for the evaluation of observer performance. MR images of patients with MC and FA were reviewed randomly. The following MR findings were assessed by the three blinded readers; margin (irregular or circumscribed); rim enhancement (present or absent); dark internal septation (absent or present); enhancing internal septation (present or absent); delayed internal enhancement (heterogeneous or homogeneous). The readers were asked to evaluate the BI-RADS MRI category using MR findings. Observer performance was determined by a receiver-operating-characteristic (ROC) curve analysis and the sensitivity, specificity, and accuracy of each MR finding was calculated. Inter-observer variability was calculated for each radiologist.

2.2.2. Statistical analysis

All statistical analyses were performed by using Ekuseru–Toukei2015 (SSRI, Tokyo, Japan). Student's t-test and Fisher's exact test were performed in the univariate analyses. Student's t-test was used to compare the mean age, diameter, and ADC values of the MCs with those of the FAs. Other findings were analyzed by using Fisher's exact test. A p value of <0.05 was considered to indicate a statistically significant difference. Multivariate logistic regression analyses were conducted with backward selection with significant findings in univariate analyses. ROC curve was fit to blinded reader's confidence rating using maximum-likelihood estimation to determine observer performance. Observer performance for each reader was estimated by calculating the area under the ROC curve (AUC). For inter-observer variability assessment in terms of interpreting images, κ statistics were used to measure the degree of agreement. A value of up to 0.20 was interpreted as slight agreement, 0.21–0.40 fair agreement, 0.41–0.60 moderate agreement, 0.61–0.80 substantial agreement, and 0.81 or greater almost perfect agreement.

3. Results

Findings of patients with MCs and FAs are presented in Table 1. In the univariate analyses, the MCs showed irregular margins more frequently than the FAs (11/27, 41% vs. 1/22, 0.5%, $p < 0.05$). The MCs also showed rim enhancement, delayed heterogeneous enhancement, and enhancing internal septation more frequently than the FAs ($p < 0.05$). The FAs showed circumscribed margins more frequently than the MCs (21/22, 95% vs. 16/27, 59%, $p < 0.05$). The FAs also showed dark internal septation more frequently than the MCs (18/22, 82% vs. 3/27, 11%, $p < 0.05$). In the multivariate analyses, the most significant feature in lesion characterization was delayed heterogeneous enhancement ($p < 0.05$). Sensitivity, specificity, and accuracy of the MR findings for differentiation of MCs and FAs in the blinded reading are summarized in Table 2. A combination of irregular margin and delayed heterogeneous enhancement showed the highest sensitivity (96.3%) and accuracy (87.8%). Enhancing internal septation showed the highest specificity (90.9%). There was no combination of findings that showed higher specificity than that of enhancing internal septation. The respective sensitivities, specificities, accuracies, and AUC for the differentiation between MCs and FAs calculated by the three radiologists are summarized in Table 3. The κ values with confidence ratings for differentiation between MCs and FAs were 0.63–0.67, which showed substantial agreement among the three radiologists.

4. Discussion

Among the BI-RADS MRI descriptors, evaluation for combination of irregular margin and delayed heterogeneous enhancement showed the highest sensitivity (96.3%) and accuracy (87.8%) for the differentiation of MCs and FAs. Some MCs showed non-circumscribed (irregular) margins in the univariate analysis (11/27, 41%) (Fig. 1). Irregular margins may indicate mixed mucinous tumors based on previous studies, which state that irregular margins on MMGs are more characteristic of mixed mucinous tumors, regardless of tumor size, and are attributable to the fibrotic and infiltrative nature of their non-mucinous component [12]. For determining internal enhancement characteristics, we used the delayed phase of dynamic CEM. Because MCs and FAs mainly tend to show persistent patterns, use of the delayed phase was thought to be more appropriate for determination of internal enhancement characteristics than use of the early phase. MCs showed delayed heterogeneous enhancement more frequently in the univariate analysis (26/27, 96%). Delayed heterogeneous enhancement showed only significant difference in the multivariate analysis. Our results showed that evaluation of irregular margin and delayed internal enhancement provides sufficient diagnostic performance, especially sensitivity for differentiation between MCs and FAs.

The kinetic pattern as the BI-RADS MRI descriptor becomes particularly helpful if the lesion has a benign morphological appearance. However, there were no significant differences in the kinetic patterns between the MCs and FAs in the univariate analysis. We found that the morphological features were more predictive than characterization of the kinetic patterns for differentiation between MCs and FA. Other authors have stated that assessment of the morphological features was more predictive in the diagnosis of breast cancer than was characterization of the kinetic curves [13,14].

The evaluation of rim enhancement as the BI-RADS MRI descriptor showed the second highest sensitivity (81.5%). MCs showed rim enhancement more frequently in the univariate analysis (25/27, 93%). However, there were 5 cases of FA that showed delayed rim enhancement in the univariate analysis. It has been reported that peripheral rim enhancement in the presence of central lesion enhancement is highly predictive of malignant disease [15,16]. Other authors have stated that no FAs with high-SI on T2-weighted images showed rim enhancement [10]. Although rim enhancement is thought to be suggestive of malignancy [15,16], benign mass lesions, such as cysts, seromas, and circumscribed fat necrosis may cause rim enhancement in addition to FA [17]. We speculated that the rim enhancement of FAs reflects their relative internal hypovascularity associated with their histopathological nature, such as fibrosis and/or hyalinization. We also speculated that, compared with the delayed phase used in another study [10], the delayed phase (240 s after the start of the IV administration) used in our study was somewhat faster and may have affected the evaluation of delayed internal enhancement.

The evaluation of dark internal septation as BI-RADS MRI descriptor showed relatively higher specificity (81.8%). Dark internal septations were more frequent in FAs (18/22, 82%) than in MCs (3/27, 11%) in the univariate analysis (Fig. 2). On the other hand, the evaluation of enhancing internal septation as non BI-RADS MRI factor showed the highest specificity (90.9%). There were more frequent enhancing internal septations in MCs (19/27, 70.4%) than in FAs (1/22, 4.5%) in the univariate analyses (Fig. 3). Although the descriptor of enhancing internal septation was eliminated in the BI-RADS MRI because of underuse, our results showed that it was a reliable descriptor for differentiation of MCs from FAs. Thus, our results are consistent with those of previous studies [10,15]. Although MCs and FAs typically have internal septation, these aspects presented differently via dynamic CEM. It has been reported that internal septations were identified within enhanc-

Table 1
Findings of patients with MCs and FAs.

	Mucinous carcinoma (27) (P-MC, 24; M-MC, 3)	Fibroadenoma (22)	Univariate		Multivariate	
			p-value[a]	OR	95%CI	*p*-value
Mean age (years)	51.7	37.8	<0.001			
Mean diameter (cm)	2.0	2.38	0.31			
≤1	1	4				
1.1–2	12	7				
>2	14	11				
Signal intensity in the T2-weighted image			0.08			
High	27	19				
Not high	0	3				
Shape			0.62			
Irregular	3	1				
Round/Oval (includes lobulated)	24	21				
Margin			0.006	15	0.0541–4128.7	0.35
Non-circumscribed (Irregular)	11	1				
Circumscribed	16	21				
Spiculated	0	0	–			
Kinetic curve pattern			0.49			
type I,						
Slow-persistent	3	3				
Medium-persistent	3	0				
Fast-persistent	15	16				
Type II, Fast-plateau	5	3				
Type III, Fast-wash-out pattern	1	0				
Rim enhancement			<0.001	12.6	0.4107–384.73	0.15
Present	25	5				
Absent	2	17				
Dark internal septation			<0.001	2.01	0.0331–122.50	0.74
Present	3	18				
Absent	24	4				
Delayed internal enhancement			<0.001	45.7	2.2706–918.06	0.01
Heterogeneous enhancement	26	6				
Homogeneous enhancement	1	16				
Enhancing internal septation			< 0.001	7.56	0.2039–280.54	0.27
Present	19	1				
Absent	8	21				
Lobulation (MC with lobulated shape, 22; FA with lobulated shape, 14)	lobulated 22 cases	lobulated 14 cases	0.08			
Strong	10	2				
Weak	12	12				
ADC value ($\times 10^{-3m}$ m^2/s)	1.465 ± 0.343	1.373 ± 0.287	0.41			

MC, mucinous carcinoma.
FA, fibroadenoma.
Type I, progressive enhancement pattern.
Type II, plateau pattern.
Type III, wash-out pattern.
ADC, apparent diffusion coefficient.
OR, odds ratio.
CI, confidence interval.
Before statistical analysis, an f-test was applied to age, diameter, and ADC values to test for a normal distribution. Age, diameter, and ADC values showed no significant difference at the 5% significance level.
[a] Student's t-test and Fisher's exact test were used.

Table 2
Sensitivity, specificity, and accuracy of the MR findings for differentiation of MCs and FAs in the blinded reading.

	Sensitivity	Specificity	Accuracy	PPV	NPV	AUC
Irregular margin	85.2	86.4	85.7	88.5	82.6	0.877
Rim enhancement	81.5	68.2	75.5	75.9	75	0.790
Dark internal septation	77.8	81.8	79.6	84	75	0.796
Enhancing internal septation	66.7	90.9	77.6	90	69	0.809
Delayed heterogeneous enhancement	81.5	86.4	83.7	88	79	0.857
Combination of irregular margin and delayed internal enhancement	96.3	77.3	87.8	84	94	0.868

Note: Sensitivity, specificity, accuracy, PPV, and NPV values are expressed as percentages.
PPV, positive-predictive value.
NPV, negative-predictive value.

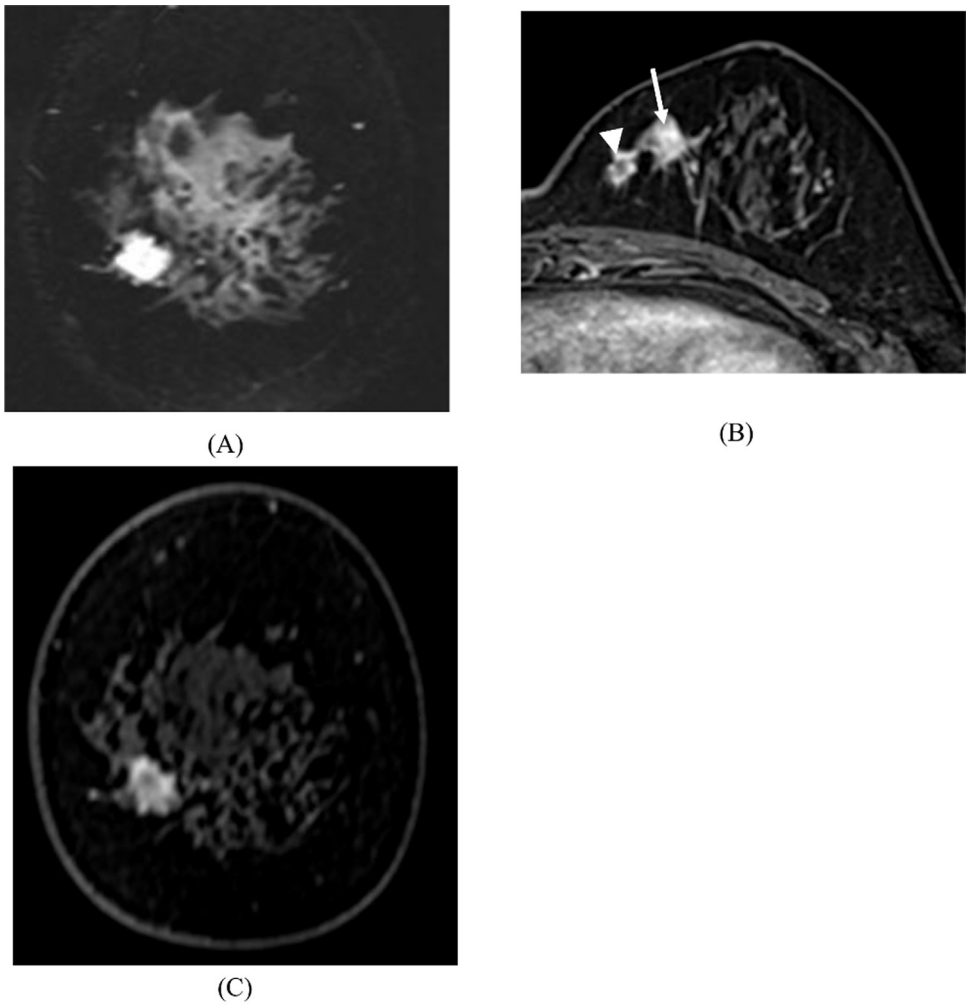

Fig. 1. Contrast-enhanced T1-weighted gradient-echo MR images of a 53-year-old woman with mucinous carcinoma (pure type) in the medial region of the left breast.
(A) Coronal T2-weighted spectral attenuated-inversion recovery image showing a high-intensity mass with a non-circumscribed margin.
Axial and (C) coronal dynamic T1-weighted Images 240 s after contrast administration (delayed phase) showing an enhancing mass measuring 13 mm along the long diameter with both a non-circumscribed margin and an irregular shape. Heterogeneous enhancement with enhancing internal septation (arrow) and a daughter lesion (arrow head) were detected.

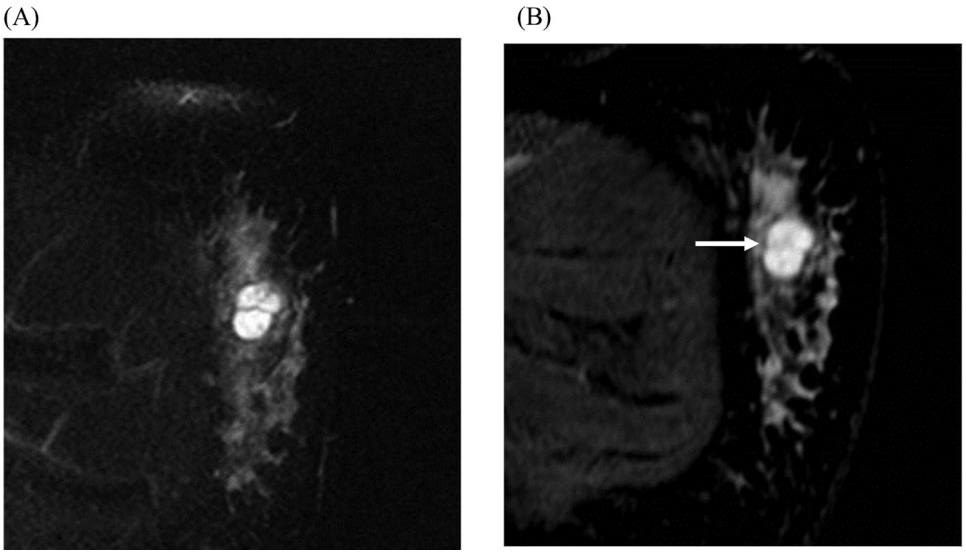

Fig. 2. Contrast-enhanced T1-weighted gradient-echo MR images of a 31-year-old woman with a fibroadenoma in the lateral region of the left breast.
(A) Coronal T2-weighted spectral attenuated-inversion recovery image showing a high-intensity mass with a circumscribed margin.
(B) Coronal dynamic T1-weighted Images 240 s after contrast administration (delayed phase) showing an enhancing mass measuring 22 mm along the long diameter with both a circumscribed margin and a lobulated shape. Homogeneous enhancement with dark internal septation was detected (arrow).

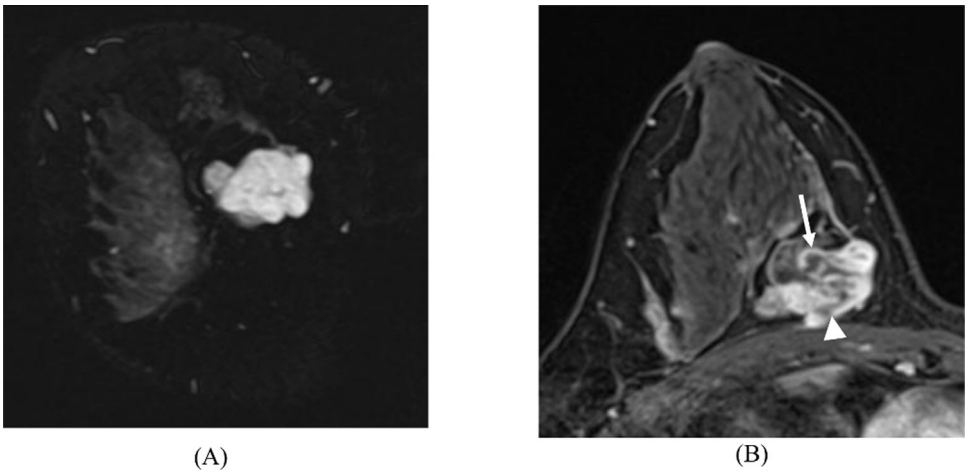

Fig. 3. Contrast-enhanced T1-weighted gradient-echo MR images of a 46-year-old woman with a mucinous carcinoma (pure type) in the medial region of the right breast. (A) Coronal T2-weighted spectral attenuated inversion recovery image showing a high-intensity mass with both a circumscribed margin and a lobulated shape. (B) Axial dynamic T1-weighted Image 240 s after contrast administration (delayed phase) showing an enhancing mass measuring 36 mm along the long diameter with both a circumscribed margin and a lobulated shape. Heterogeneous enhancement (arrow head) with enhancing internal septation (arrow) are shown.

Table 3
Sensitivity, specificity, and accuracy for three readers.

	Reader 1	Reader 2	Reader 3
Sensitivity	81.5	85.2	88.9
Specificity	90.9	81.8	86.4
Accuracy	85.7	83.7	87.8
AUC	0.858	0.832	0.874
p-value	<0.001	<0.001	<0.001

Note: Sensitivity, specificity, and accuracy values are expressed as percentages.

ing FAs and appeared to correlate with collagenous bands on histopathological analysis [7]. We speculated that the hypovascular nature of collagenous bands of FAs caused the dark internal septation. MCs are composed of "aggregates of tumor cells" surrounded completely by mucin and compartmentalized by fibrovascular bands [18]. We speculated that enhancing internal septations are related to fibrovascular bands within the MCs. Our results regarding enhancing internal septations are consistent with those of previous studies; it has been reported that enhancing septation demonstrated on dynamic CEM was a characteristic finding of MCs in high-SI breast tumors on T2-weighted images [10].

For signal intensity in the T2-weighted image as non BI-RADS MRI factor, all MCs were detected as high-SI lesions on T2-weighted images, which suggests that high-SI on T2-weighted images is characteristic of P-MCs or M-MCs similar to P-MCs. On the other hand, three FAs were detected as not high-SI on T2-weighted image. We thought the reason of this were associated with their histopathological change, such as fibrosis and/or hyalinization.

The ADC values of breast tumors as non BI-RADS MRI factor are inversely correlated with tumor cellularity [19]. No significant difference in ADC values was found between the MCs and FAs in the present study; this finding was thought to be because of the T2 shine-through effect. On diffusion-weighted imaging (DWI), an internal structure with heterogeneous high SI and nodular architecture together with a hypointense lesion may be additional signs of MC, although these findings may not always be observed [20]. In the present study, the internal appearance of the lesions on DWI was not evaluated, but evaluation of the internal texture of the lesion on DWI other than by ADC mapping may be a diagnostic aid for differentiation of MCs from FAs.

Our study had some limitations. The small sample size limited the extent of analysis. The study was also retrospective, and some selection bias may have been present. Many typical FAs diagnosed on US and/or MRI in our institution were not always indicated for biopsy or surgical resection. In some cases, US was performed on these tumors for the purpose of close inspection, but MRI is often omitted because of the smaller size and/or lack of enlargement tendency of the tumors. Third, MCs were closely investigated in a pathological study. On the other hand, FAs were not investigated sufficiently to prove the internal characteristics. Therefore, there is no conclusive evidence showing that other pathological changes, except for myxoid or edematous changes, were present or not.

5. Conclusion

We evaluated the latest BI-RADS MRI (5th edition) descriptors and additional non BI-RADS MRI factors that contribute to differentiation between P-MCs or M-MCs similar to P-MCs and FAs. All of the findings were retrospectively evaluated by one radiologist. Univariate analyses showed that the presence of a circumscribed margin and dark internal septation were characteristic of FAs. The presence of an irregular margin, rim enhancement, delayed heterogeneous enhancement, and enhancing internal septation were more frequently observed in MCs than in FAs. In multivariate analyses, the most significant features in lesion characterization was delayed heterogeneous enhancement. Then, three radiologists blinded to clinical and histopathological information retrospectively reviewed the MR images by using MR findings that showed a significant association with outcome in the univariate analyses. Combination of irregular margin and delayed heterogeneous enhancement showed the highest sensitivity (96.3%) and accuracy (87.8%). Enhancing internal septation showed the highest specificity (90.9%); therefore, this characteristic can be used to help differentiate P-MCs or M-MCs similar to P-MCs from FAs in breast cancer patients.

Conflicts of interest

None.

Acknowledgement

The authors wish to thank Fumitoshi Kodaka M.D., Ph.D for comments on statistical analyses of this paper.

References

[1] S.Y. Bae, M.Y. Choi, D.H. Cho, J.E. Lee, S.J. Nam, J.H. Yang, Mucinous carcinoma of the breast in comparison with invasive ductal carcinoma: clinicopathologic characteristics and prognosis, J. Breast Cancer 14 (2011) 308–313.

[2] S. Di Saverio, J. Gutierrez, E. Avisar, A retrospective review with long term follow up of 11,400 cases of pure mucinous breast carcinoma, Breast Cancer Res. Treat. 111 (2008) 541–547.

[3] K. Komaki, G. Sakamoto, H. Sugano, T. Morimoto, Y. Monden, Mucinous carcinoma of the breast in Japan: a prognostic analysis based on morphologic features, Cancer 61 (1988) 989–996.

[4] S. Monzawa, M. Yokokawa, T. Sakuma, S. Takao, K. Hirokaga, K. Hanioka, et al., Mucinous carcinoma of the breast: MRI features of pure and mixed forms with histopathologic correlation, Am. J. Roentgenol. 192 (2009) W125–31.

[5] J.Z. Tan, J. Waugh, B. Kumar, J. Evans, Mucinous carcinomas of the breast: imaging features and potential for misdiagnosis, J. Med. Imaging Radiat Oncol. 57 (February) (2013) 25–31.

[6] R. Yamaguchi, M. Tanaka, Y. Mizushima, Y. Hirai, M. Yamaguchi, H. Terasaki, et al., High-grade acellular carcinoma and matrix-producing carcinoma of the breast: correlation between ultrasonographic findings and pathological features, Med. Mol. Morphol. 44 (2011) 151–157.

[7] M.G. Hochman, S.G. Orel, C.M. Powell, M.D. Schnall, C.A. Reynolds, L.N. White, Fibroadenomas: MRImaging appearances with radiologic-histopathologic correlation, Radiology 204 (1997) 123–129.

[8] S.G. Orel, M.D. Schnall, V.A. LiVolsi, R.H. Troupin, Suspicious breast lesions: MR imaging with radiologic-pathologic correlation, Radiology 190 (1994) 485–493.

[9] C.K. Kuhl, S. Klaschik, P. Mielcarek, J. Gieseke, E. Wardelmann, H.H. Schild, Do T2-weighted pulse sequences help with the differential diagnosis of enhancing lesions in dynamic breast MRI, J. Magn. Reson. Imaging 9 (1999) 187–196.

[10] S. Yuen, T. Uematsu, M. Kasami, K. Tanaka, K. Kimura, J. Sanuki, et al., Breast carcinomas with strong high-signal intensity on T2-weighted MR images: pathological characteristics and differential diagnosis, J. Magn. Reson. Imaging 25 (2007) 502–510.

[11] E. Morris, C. Comstock, C. Lee, et al., Magnetic resonance imaging, in: Breast Imaging Reporting and Data System, American College of Radiology, Reston, VA, 2013, ACR BI-RADS® atlas.

[12] T.E. Wilson, M.A. Helvie, H.A. Oberman, L.K. Joynt, Pure and mixed mucinous carcinoma of the breast: pathologic basis for differences in mammographic appearance, Am. J. Roentgenol. 165 (1995) 285–289.

[13] M.D. Schnall, J. Blume, D.A. Bluemke, G.A. DeAngelis, N. DeBruhl, S. Harms, et al., Diagnostic architectural and dynamic features at breast MR imaging: multicenter study, Radiology 238 (2006) 42–53.

[14] M.C. Mahoney, C. Gatsonis, L. Hanna, W.B. DeMartini, C. Lehman, Positive predictive value of BI-RADS MR imaging, Radiology 264 (2012) 51–58.

[15] L.W. Nunes, M.D. Schnall, E.S. Siegelman, C.P. Langlotz, S.G. Orel, D. Sullivan, et al., Diagnostic performance characteristics of architectural features revealed by high spatial-resolution MR imaging of the breast, Am. J. Roentgenol. 169 (1997) 409–415.

[16] M. Kobayashi, H. Kawashima, O. Matsui, Y. Zen, M. Suzuki, M. Inokuchi, et al., Two different types of ring-like enhancement on dynamic MR imaging in breast cancer: correlation with the histopathologic findings, J. Magn. Reson. Imaging 28 (2008) 1435–1443.

[17] I. Millet, E. Pages, D. Hoa, S. Merigeaud, F. Curros Doyon, X. Prat, et al., Pearls and pitfalls in breast MRI, Br. J. Radiol. 85 (2012) 197–207.

[18] F.A. Tavassoli, Pathology of The Breast, McGraw Hill Professional, 1999.

[19] M. Hatakenaka, H. Soeda, H. Yabuuchi, Y. Matsuo, T. Kamitani, Y. Oda, et al., Apparent diffusion coefficients of breast tumors: clinical application, Magn. Reson. Med. Sic. 7 (2008) 23–29.

[20] R. Woodhams, S. Ramadan, P. Stanwell, S. Sakamoto, H. Hate, M. Ozaki, et al., Diffusion-weighted imaging of the breast: principles and clinical applications, Radiographics 31 (2011) 1059–1084.